RSC Advances

PAPER

View Article Online
View Journal | View Issue

Cite this: *RSC Adv.*, 2022, **12**, 4828

Lanthanide induced variability in localised Co^{II} geometries of four triangular $L_3Co_3^{II}Ln^{III}$ complexes†

Tyson N. Dais, [a] Rina Takano,[b] Takayuki Ishida [b] and Paul G. Plieger *[a]

Four tetranuclear heterobimetallic triangle complexes $[L_3Co_3Dy(NO_3)_2(H_2O)(MeOH)_5](NO_3)$ (**C1**), $[L_3Co_3Gd(NO_3)_3(MeOH)_4]$ (**C2**), $[L_3Co_3La(NO_3)_2(H_2O)_6](NO_3)(H_2O)$ (**C3**), and $[L_3Co_3TbCl(NO_3)_2(H_2O)_{0.5}(MeOH)_{3.5}]$ (**C4**), where H_2L = 1,4-bisformylnaphthalene-2,3-diol, have been synthesised and structurally characterised. Each complex crystallises with a complete molecule in the asymmetric unit ($Z' = 1$) and displays near perfect octahedrality in two out of three Co^{II} centres. The third Co^{II} ion assumes a different coordination geometry in each complex: six-coordinate octahedral in **C1**, six-coordinate with a distortion towards trigonal prismatic in **C2**, five-coordinate trigonal bipyramidal in **C3**, and five-coordinate square pyramidal in **C4**; which has been attributed to increasing lanthanide cation size, coupled with a non-macrocyclic coordination environment. Continuous Shape Measurement (CShM) calculations and octahedral distortion parameter calculations were performed, using the SHAPE and OctaDist software packages, respectively, in order to aid in the assessment of each metal centre's local coordination geometry. The preliminary magnetic investigation of **C3** found $\chi_m T = 9.4$ cm^3 K mol^{-1} at 300 K and $M = 7.1$ μ_B at 1.8 K, which are approximately two thirds the maximum theoretical values for three Co^{II} ions and indicates the presence of a relatively large zero-field splitting parameter ($D/k_B = 65$ K) operative in each Co^{II} ion rather than exchange coupling between the Co^{II} centres.

Received 2nd December 2021
Accepted 1st February 2022

DOI: 10.1039/d1ra08797e

rsc.li/rsc-advances

Introduction

Metal ions have a rich history in aiding otherwise untenable chemical transformations and play a pertinent role in the self-assembly process of many molecular clusters. Of particular importance, is the use of metals to template the formation of macrocycles and interlocked molecules in a controlled and predictable manner.[1–8] While mononuclear and homometallic polynuclear complexes are among the most common, there is a great interest in heterometallic complexes with predictable nuclearities and topologies. Heterometallic polynuclear complexes have been explored in many fields of science from antibacterial agents[9–11] and molecular machines,[12–15] to heterogenous catalysts,[16–19] molecular magnets,[20–25] and spintronic devices.[26–30]

A hexa-phenolate macrocycle, templated with an all-in-plane tetranuclear Zn_3LaO_6 3d/4f core, was first reported by Nabeshima.[31] This metal cation templated route provided a vast improvement in yield over their previous metal-free attempts to perform 3 + 3 Schiff base condensations of 1,4-diformylbenzene-2,3-diol with various diamine linkers.[32] This same method involving templated macrocyclisation was later extended to include various combinations of trivalent lanthanide ions with Zn^{II},[33–40] Cu^{II},[41–46] Ni^{II},[47] or Co^{II} centres.[48] Families of triangular macrocyclic complexes containing Zn^{II}, Cu^{II}, and Ni^{II} with a variety of Ln^{III} have been investigated by Brooker *et al.* for their magnetic properties.[33,34,41–47] More recently, Mashima and Nozaki *et al.* have prepared macrocyclic complexes with a $Co^{II}_3Ln^{III}O_6$ core for the catalysis of copolymerisation of CO_2 and cyclohexene oxide.

While some of the complexes discussed in these reports have been structurally characterised, many have not. In particular, the aldehyde containing intermediate complexes which self-assemble prior to condensation/macrocyclisation have only been successfully isolated, with full structural characterisation reported, for three older examples (Refcodes: HICLIP[31] and XUVVIV/XUVVOB[47]) and four recently reported Ni_3Ln examples (WARKIN, WARKEJ, WARKOT, and WARKUZ).[49]

MacLachlan *et al.*[50] established a method to obtain heptanuclear Zn^{II} clusters from the reaction of a pre-formed macrocyclic hexa-phenolate ligand with seven equivalents of $Zn(OAc)_2 \cdot 2H_2O$, which was later shown to be capable of forming the Zn_3LaO_6 type complex by Nabeshima *et al.*[51] Nabeshima further showed that the 3 + 3 condensation reaction can be

[a]*School of Natural Sciences, Massey University, Private Bag 11 222, Palmerston North, New Zealand. E-mail: p.g.plieger@massey.ac.nz*

[b]*Department of Engineering Science, Graduate School of Informatics and Engineering, The University of Electro-Communication, 1-5-1 Chofugaoka, Chofu, Tokyo 182-8585, Japan*

† Electronic supplementary information (ESI) available. CCDC 2105529–2105532. For ESI and crystallographic data in CIF or other electronic format see DOI: 10.1039/d1ra08797e

carried out in the presence of two equivalents of zinc per equivalent dialdehyde, yielding a hexanuclear complex contained within the expected macrocycle.[31]

While following our interest in exploring the magneto–structural correlations of non-macrocyclic dialdehyde ligated TM_3Ln type complexes, four $Co^{II}{}_3Ln$ complexes have been synthesised with notably different Co^{II} coordination geometries. We now report the self-assembly and structural characterisation of four non-macrocyclic triangle complexes containing $Co^{II}{}_3Ln^{III}O_6$ cores, each of which features two octahedrally coordinated Co^{II} centres and a third Co^{II} featuring a variation in geometry. Preliminary magnetic measurements have been carried out on the La^{III} containing complex, **C3**, and are briefly discussed.

Results and discussion

The four L_3Co_3Ln complexes reported here were prepared from a 3 : 1 : 3 mixture of methanolic solution of cobaltous nitrate, a lanthanide salt, and the relatively simple ligand, 1,4-bisformylnaphthalene-2,3-diol (H_2L). Addition of the cobalt solution caused rapid dissolution of the ligand suspension regardless of order, the same effect was not observed when the lanthanide solution was added prior to the cobalt solution. The reaction mixture required stirring overnight as the reaction proceeded through a (non-product) precipitation stage which redissolved upon further stirring. The lanthanide salts utilised were $Dy(NO_3)_3\cdot 6H_2O$ (**C1**), $Gd(NO_3)_3\cdot 6H_2O$ (**C2**), $La(OAc)_3\cdot 6H_2O$ (**C3**), and $TbCl_3\cdot 6H_2O$ (**C4**). While these complexes initially appeared to be stable in air, the crystallinity of some samples was observed to be fragile to desolvation.

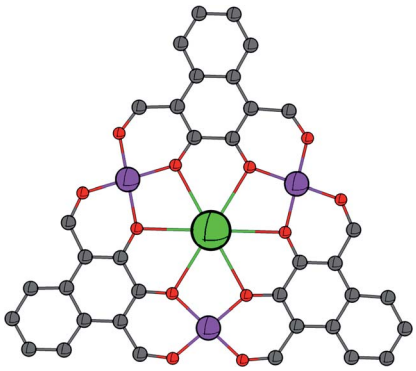

Fig. 1 Schematic showing the general metal–ligand connectivity of the complexes reported in this work. C = grey, O = red, Co^{II} = purple, and Ln^{III} = green.

Each lanthanide is bound equatorially in an O_6 environment by three catecholate (equivalent to six phenolate) groups in an approximately planar arrangement, selected distances and angles can be found in Table 1. The prearrangement of the three ligand molecules around the lanthanide centre brings the aldehyde groups into proximity akin to the imine nitrogens of a salen moiety (Fig. 1). The two adjacent aldehyde and phenolate groups form an O4 environment to bind to the equatorial sites of the cobalt centres while the remaining axial coordination sites of each metal are bound by a mixture of solvent molecules or anions. Complexes **C1–C3** all crystallised in the triclinic space group $P\bar{1}$, while complex **C4** crystallised in the monoclinic space group $C2/c$. Only **C1** and **C2** contain three 6-coordinate Co^{II} centres, with **C3** and **C4** each containing one heavily distorted 5-coordinate Co^{II} centre. Of the four structurally characterised $Co^{II}{}_3Ln$ type complexes reported by Mashima and Nozaki *et al.*[48] all but one Co^{II} centre has near perfect octahedral geometry. A single Co^{II} ion in the Co_3Ce complex features a near square-pyramidal geometry. In order to assess the local coordination geometry of each Co^{II} centre, Continuous Shape Measurement (CShM) calculations[52,53] were employed alongside octahedral distortion calculations ($\langle D\rangle$, Δ, ζ, and Σ)

Table 1 Selected bond lengths and angles for **C1–C4**

Distance/Å	C1	C2	C3	C4
Ln^{III}–O_{phenol}	2.393(8)–2.460(8)	2.410(5)–2.552(6)	2.567(9)–2.657(8)	2.439(5)–2.546(5)
Ln^{III}–$O_{nitrate}$	2.450(8)–2.459(7)	2.455(6)–2.498(5)	2.625(8)–2.801(9)	2.438(6)–2.494(5)
Ln^{III}–$O_{solvent}$ [a]	2.339(7)	—	2.576(9)	—
Co^{II}–O_{phenol}	1.980(8)–2.036(9)	1.989(5)–2.011(5)	1.984(8)–2.046(8)	1.984(5)–2.045(5)
Co^{II}–O_{formyl}	1.996(9)–2.044(10)	1.990(8)–2.046(5)	1.982(9)–2.044(9)	1.988(5)–2.025(4)
Co^{II}–O_{water}	2.148(9)	—	1.922(13)–2.177(8)	2.195[c]
Co^{II}–$O_{methanol}$	2.133(8)–2.191(8)	2.108(6)–2.178(6)	—	2.133(6)–2.200(20)[c]
Co^{II}–Anion[b]	2.166(8)	2.130(5)–2.206(6)	—	2.292(2)
Av. Co^{II}–Co^{II}	6.248(4)	6.365(2)	6.392(3)	6.353(2)
Av. Co^{II}–Ln^{III}	3.610(3)	3.676(2)	3.706(2)	3.671(1)
Min. Ln^{III}–Ln^{III}	10.221(2)	10.625(2)	9.598(1)	10.540(1)
Ln^{III}–Co_3 plane	0.139(2)	0.091(1)	0.333(1)	0.143(1)
Co4–O_4 plane[d]	0.015(5)	0.648(3)	0.609(5)	0.581(3)
Angle/°				
Co^{II}–O–Ln^{III}	106.2(4)–109.3(4)	106.2(2)–111.0(2)	104.1(3)–108.5(3)	107.0(2)–109.2(2)

[a] $O_{methanol}$ (**C1**) and O_{water} (**C3**). [b] Anion is μ_1-NO_3 (**C1**), μ_2-NO_3 (**C2**), μ_1-Cl (**C4**). [c] The Co2 cap in **C4** has been modelled as a 1 : 1 disordered methanol/water cap. [d] The O_4 plane corresponds to the least-squares plane of the four ligand-based (equatorial) donors in the idealised octahedral binding environment.

using the OctaDist software package,[54] the values of these parameters can be found in Table 2.

Molecular structures

Crystal structure and refinement details for **C1–C4** can be found in Table S1 of the ESI.†

The crystal structure of **C1** (Fig. 2) shows the complex takes a non-planar arrangement and is the only complex reported here to contain three near perfect six-coordinate octahedral Co^{II} centres with CShM(OC-6)/Σ values of 1.586/66.70 (Co2), 1.634/68.80 (Co3), and 0.733/38.29 (Co4).

The Dy^{III} centre of **C1** occupies a nine-coordinate environment where the three non-equatorial donors are an axially coordinated methanol and an axially coordinated μ_2-NO_3 group, binding opposite sides of the Co_3 plane. The Co2 and Co3 cobalt centres of **C1** are axially capped with solvent type molecules, whereas Co4 features an axially coordinated μ_1-NO_3 group as well as a methanol cap. In order to achieve charge neutrality, the total metal charge of +9 (Dy^{3+} and 3 × Co^{2+}) is partially balanced by 3 × L^{2-} and the two coordinated NO_3^- groups, with the final negative charge originating from a non-coordinated NO_3^- anion, giving an overall formula of $[L_3Co_3Dy(NO_3)_2(H_2O)(MeOH)_5](NO_3)$. **C1** features extensive intermolecular and intra-complex hydrogen bonding (Fig. 3). The non-coordinated nitrate group forms strong hydrogen bonds from its O26 oxygen to a methanol cap of Co2 (O26···H13 = 1.989(10) Å) and the water cap of Co3 (O26···H15A = 1.904(10) Å). A symmetry generated complex provides two further hydrogen bonds, stemming from the H14* proton of a methanol cap of Co2* (O27···H14* = 2.496(9) Å, and O28···H14* = 2.100(8) Å). There are also two strong hydrogen bonds formed between the two units complex by the methanol cap of Co4* with the water cap of Co3 (O15···H17* = 2.008(7) Å), and the proton of the Co3 water cap acting as a hydrogen bond donor

Table 2 Calculated parameters describing distortion of the coordination sphere from the ideal octahedral geometry[c]

	OC-6[a]	⟨D⟩	Δ	ζ	Σ
C1–Co2	1.586	2.0693	0.3499	0.00091	66.701
C1–Co3	1.634	2.0690	0.2849	0.00061	68.799
C1–Co4	0.733	2.0589	0.4800	0.00174	38.287
C2–Co2	1.263	2.0529	0.3597	0.00106	59.272
C2–Co3	0.301	2.0522	0.3569	0.00095	29.476
C2–Co4[b]	4.914	2.0612	0.4273	0.00154	115.791
C3–Co2	0.355	2.0683	0.3929	0.00114	28.613
C3–Co3	0.605	2.0553	0.2738	0.00073	43.621
C4–Co2	0.738	2.0545	0.3429	0.00089	43.664
C4–Co4	0.947	2.0595	0.4181	0.00137	56.121

[a] Values near or below one indicate minimal distortion from the ideal geometry. [b] **C2**–Co4 is distorted towards D_{3h} trigonal prismatic. [c] The octahedral distortion parameters calculated by OctaDist are defined as: ⟨D⟩, the average M–L bond length; Δ, the average of the deviations of M–L bond lengths from ⟨D⟩; ζ, the sum of the deviation of bond lengths from ⟨D⟩; and Σ, the sum of deviations of the 12 *cis* angles from 90°.

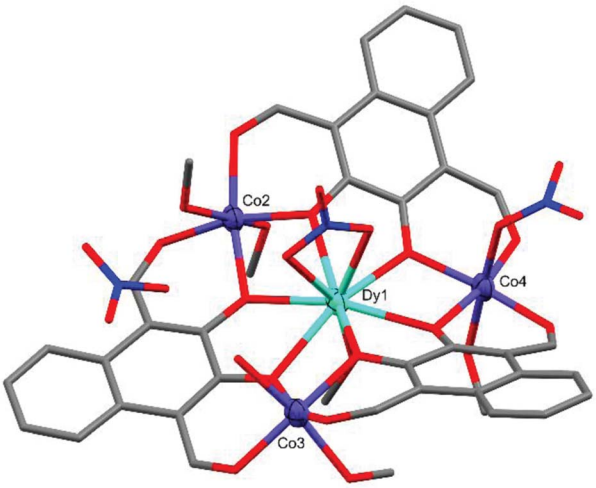

Fig. 2 X-ray crystal structure of **C1**. Thermal ellipsoids of metal atoms shown at 70% probability. H atoms have been omitted for clarity. C = grey, O = red, N = blue.

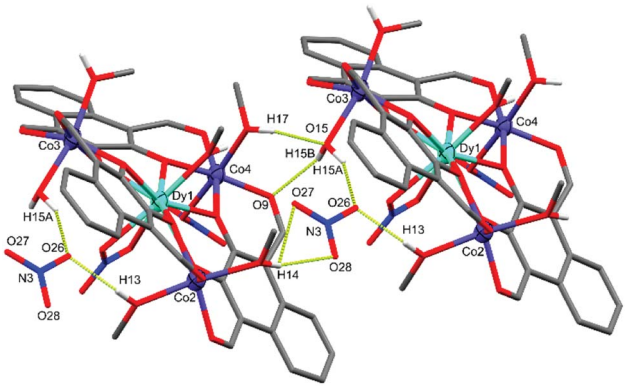

Fig. 3 X-ray crystal structure of **C1** showing the intermolecular hydrogen bonding between two units complex and the non-coordinated nitrate. Thermal ellipsoids of metal atoms shown at 70% probability. Non-acidic H atoms have been omitted for clarity. H bonds shown as segmented yellow bonds. C = grey, O = red, N = blue.

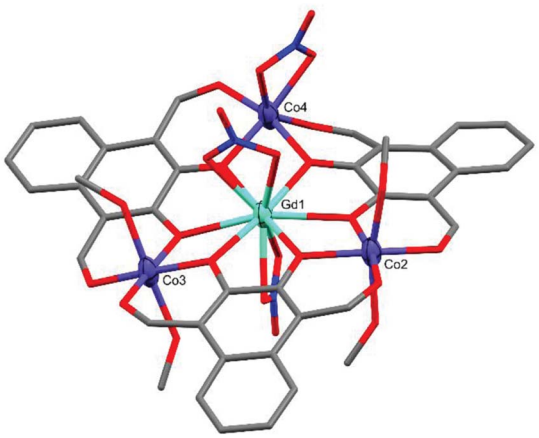

Fig. 4 X-ray crystal structure of **C2**. Thermal ellipsoids of metal atoms shown at 70% probability. H atoms have been omitted for clarity. C = grey, O = red, N = blue.

to the aldehyde binding Co4* in the symmetry generated molecule (O9*···H15B = 2.078(8) Å).

Complex **C2** crystallised in the triclinic space group $P\bar{1}$ with the formula $[\mathbf{L}_3Co_3Gd(MeOH)_4(NO_3)_3]$ (Fig. 4). **C2** is significantly more planar than **C1** and features two near perfectly octahedral cobalt centres (Co2 and Co3) each axially coordinated by two methanol molecules with CShM(OC-6)/Σ values of 1.263/59.27 (Co2) and 0.301/29.48 (Co3). The remaining cobalt centre, Co4, is also six-coordinate but is capped by a μ_2-NO_3 group leading to a heavily distorted octahedral geometry tending towards D_{3h} trigonal prismatic with CShM(OC-6, TPR-6)/Σ values of 4.914, 9.173/115.79. At the heart of **C2** is a ten-coordinate Gd^{III} ion, capped either side of the Co_3 plane by a μ_2-NO_3 group, with a *pseudo*-hexagonal bipyramidal coordination geometry.

Similar to **C1** and **C2**, complex **C3** (Fig. 5) also crystallised in $P\bar{1}$, with the formula $[\mathbf{L}_3Co_3La(NO_3)_2(H_2O)_6](NO_3)(H_2O)\cdot[1.5\ Et_2O]$, but only has two six-coordinate cobalt centres (Co2 and Co3). Both Co2 and Co3 are axially coordinated by water molecules forming near perfect octahedral coordination geometries with CShM(OC-6)/Σ values of 0.355/28.61 (Co2) and 0.605/43.62 (Co3). In contrast, Co4 has only a single axially coordinated water molecule resulting in a five-coordinate distorted D_{3h} trigonal bipyramidal coordination geometry with a CShM(TBPY-5) value of 1.678.

The La^{III} ion in the centre of **C3** is coordinated by two μ_2-NO_3 groups and a water molecule, resulting in an 11-coordinate centre with the approximate C_{5v} symmetry of a capped pentagonal antiprism with a CShM(JCPAPR-11) value of 4.655. The final negative charge required to balance the +9 charge of the metal centres, as in **C1**, is present as a non-coordinated nitrate. This non-coordinated nitrate species is crystallographically disordered over two spatially similar sites with freely refined occupancies of 0.47(2) (site A) and 0.53(2) (site B) (Fig. 6, inset). A water cap of Co3 forms strong hydrogen bonds to three of the four possible oxygen atoms belonging to the disordered nitrate (setting the cut-off distance to 2.50 Å). The inset of Fig. 6 shows

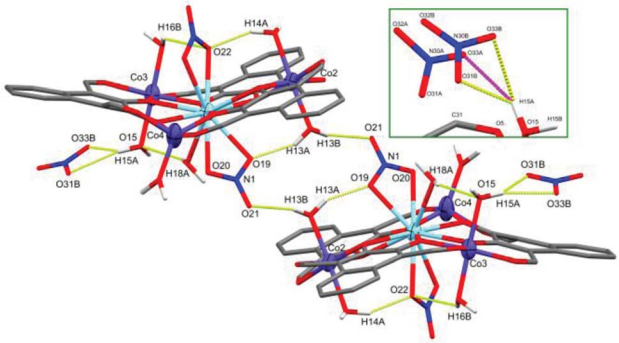

Fig. 6 X-ray crystal structure of **C3** showing the intermolecular hydrogen bonding between two units complex and the non-coordinated nitrate. Inset showing the two partial occupancy nitrate sites. Thermal ellipsoids of metal atoms shown at 70% probability. Non-acidic H atoms have been omitted for clarity. H bonds shown as segmented yellow/pink bonds. C = grey, O = red, N = blue.

both non-coordinated nitrate sites and the hydrogen bonds they form with H15A: O31B···H15A = 1.848(9) Å, O33B···H15A = 2.281(9) Å, and O33A···H15A = 2.154(9) Å, with an O31A···H15A distance of 2.905(8) Å.

A second unit complex is generated by inversion symmetry (Fig. 6) which forms a symmetric set of hydrogen bonds between the N1 nitrate cap of La1 and O13 water cap of Co2 in each unit complex, resulting in an intramolecular hydrogen bond (O19···H13A = 1.936 Å) and an intermolecular hydrogen bond (O21*···H13B = 1.951 Å). The crystal structure of **C3** was also found to contain diethyl ether molecules across at least 4 sites in the asymmetric unit. These lattice solvents were heavily disordered and unstable even to isotropic refinement, thus have been modelled within a solvent mask using the Olex2 implementation of BYPASS, containing 64 electrons in 192 $Å^3$ per asymmetric unit which fits well with 1.5 diethyl ether molecules (63 electrons). These solvate species were not observed in the

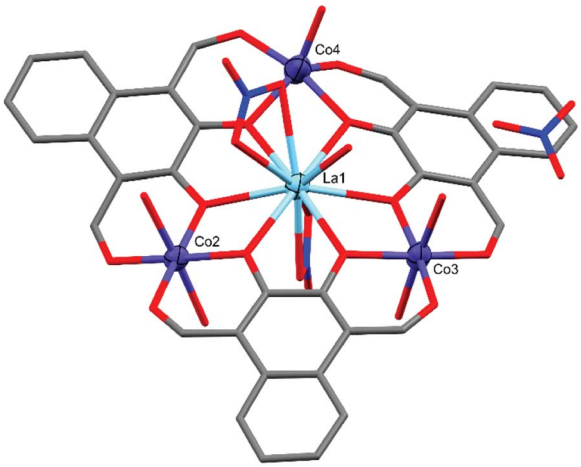

Fig. 5 X-ray crystal structure of **C3**. Thermal ellipsoids of metal atoms shown at 70% probability. H atoms and disordered species have been omitted for clarity. C = grey, O = red, N = blue.

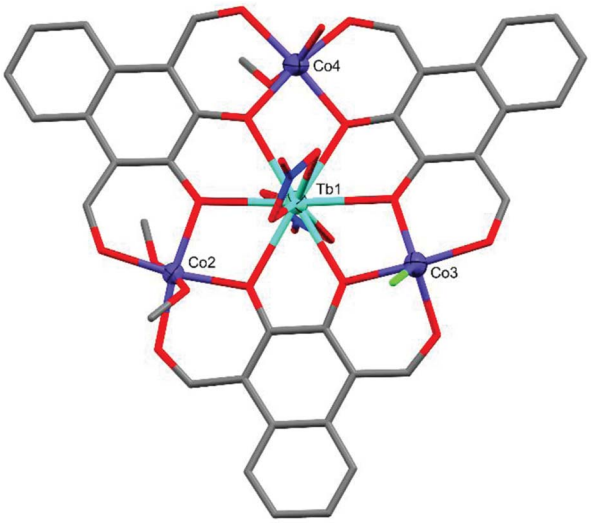

Fig. 7 X-ray crystal structure of **C4**. Thermal ellipsoids of metal atoms shown at 70% probability. H atoms and disordered species have been omitted for clarity. C = grey, O = red, N = blue, Cl = green.

microanalytical data, but are consistent with the observation of the crystalline sample rapidly crumbling upon sitting in air.

The crystal structure of **C4** (Fig. 7) revealed a relatively non-planar system featuring one five-coordinate and two six-coordinate cobalt centres. Although the preparation of **C3** reported here also utilised a non-nitrate lanthanide salt ($La(OAc)_3 \cdot 6H_2O$), **C4** exclusively features a mixture of nitrate and non-nitrate (chloride) anions. Both Co2 and Co3 are octahedral, with CShM(OC-6)/Σ values of 0.738/43.66 (Co2) and 0.947/56.12 (Co4), with Co4 being axially coordinated by two methanol molecules. Co2 has an axially coordinated methanol on one side of the plane, however the other cap is present as a crystallographically disordered 1 : 1 methanol/water species. Co3 is unambiguously capped by a single chloride anion originating from the $TbCl_3 \cdot H_2O$ salt with an overall formula of $[\mathbf{L}_3Co_3TbCl(NO_3)_2(H_2O)_{0.5}(MeOH)_{3.5}] \cdot [2.5H_2O]$. This five-coordinate cobalt centre sits in an approximately C_{4v} square pyramidal coordination geometry with a CShM(SPY-5) value of 1.734.

The crystal lattice was found to contain two solvent accessible voids equivalent to 14 electrons in 68 $Å^3$ and 8 electrons in 24 $Å^3$ when modelled within a solvent mask using Olex2, which corresponds to approximately 1.5 water molecules and 1 water molecule, respectively, per asymmetric unit and is consistent with the microanalytical data for **C4** – see experimental details.

Based on the general formulation $\mathbf{L}_3Co_3Ln(anion)_3$ + solvents, cobalt is expected to be in the +2 oxidation state (+3 from Ln^{III}, −2 from **L**, and −1 from each anion, giving an overall charge of −6 to be balanced by three cobalt centres). The same result is evidenced by further examining the average equatorial Co–O bond lengths in Table 1, which are consistent with the longer bonds expected for Co^{II}. Further, the bond valency[55,56] of each cobalt centre has been assessed in PLATON[57,58] and all sit in the range of 2.18–2.36.

The structural differences between the four complexes are quite striking and in the first instance may be attributed to the differing sizes of the central lanthanide cation. For instance, the structure of **C1**, with a small Dy^{III} ion at its centre, is dictated by the cobalt centres, each one adopting an ideal octahedral geometry. The differences between the larger lanthanide cations in complexes **C2–C4** is more subtle, with no clear or obvious reason for the different cobalt geometries, other than they are now unable to form idealised octahedral geometries.

π–π stacking interactions were analysed in Olex2 (ref. 59) with aromatic centroid–centroid distances listed in Table 3 as well as the cross-sectional molecular area, calculated in the Co_3–$\mathbf{L}_3$ plane using the inbuilt ChemCraft utility.

Table 3 Calculated π–π stacking distances and cross-sectional area

Complex	π–π stacking (Å)	Molecular area ($Å^3$)
C1	3.763–3.824	206.5
C2	3.731–3.740	208.9
C3	3.586–3.955	213.1
C4	3.551–3.791	212.1

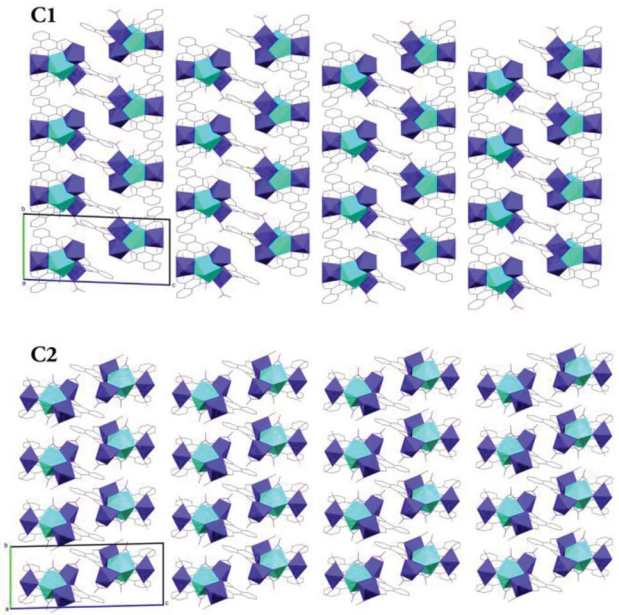

Fig. 8 Simplified X-ray crystal structure packing diagrams of **C1** and **C2** viewed along the crystallographic *a*-axis.

Complex **C3**, containing the largest trivalent lanthanide ion (La^{III}), has the largest calculated molecular area as well as the longest range π–π stacking interaction (as determined by Olex2). It also features the longest average Co^{II}–Ln^{III} and Co^{II}–Co^{II} distances, however it interestingly also has the shortest Ln^{III}–Ln^{III} distance (Table 3). The same trend in ionic radii *vs.* cross-sectional molecular area is not followed for the other three complexes. Complex **C4** contains Tb^{III} which is smaller than Gd^{III} (**C2**) but larger than Dy^{III} (**C1**), however **C4** has the second largest calculated molecular area which may be attributed to the way in which the chloride cap of Co3 in **C4** influences the planarity and shape of the complex and hence the crystal packing.

The crystal packing diagrams of **C1** and **C2** viewed along the crystallographic *a*-axis (Fig. 8) show that these complexes pack similar to a two-dimensional layered system along the *ab*-plane with clear inter-layer separations along the *c*-axis. Although **C3** has the same metric symmetry and space group as **C1** and **C2**, the geometry of the unit cell is considerably different. Where **C1** and **C2** have similar lengths in *a* and *b* and both *α* and *β* angles are near 90°, **C3** has similar lengths in *b* and *c* with the corresponding *α* and *γ* angles being near 90°. The shorter length of *c* in **C3** relative to the other two triclinic structures results in a greater proportion of a third molecule, whose centre of mass sits outside of the unit cell, occupying the space to ensure $Z = 2$.

Magnetic measurement

The DC magnetic susceptibility and magnetisation measurements have been performed to examine the potential Co–Co interactions and/or zero-field splitting effects present within this complex. As complexes **C1–C4** each feature a Co^{II} centre

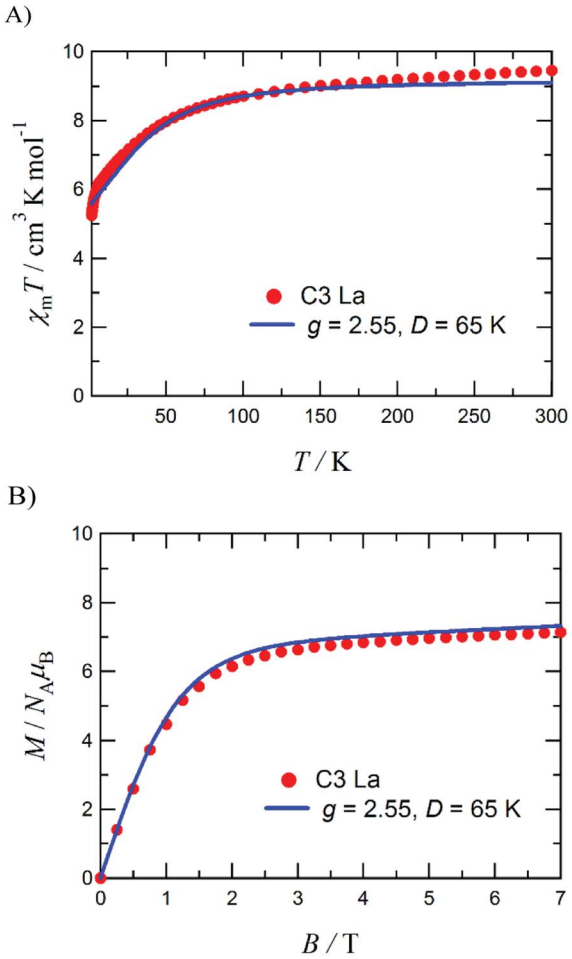

Fig. 9 Plot of $\chi_m T$ *vs.* T for **C3** measured at 0.5 T (A) and the M *vs.* H plot for **C3** measured at 1.8 K (B), including fits and parameters. Measurements were performed on a polycrystalline sample fixed in a small amount of eicosane.

with different coordination geometries, this initial study of **C3** is not necessarily representative of the other three complexes.

Fig. 9A shows the $\chi_m T$ product reaching 9.4 cm^3 K mol^{-1} at 300 K, which clarified the presence of three $S_{Co^{II}} = 3/2$ spins with $g = 2.59$. The experimental magnetisation (Fig. 9B) at 7 T was 7.1 μ_B, which corresponds to *ca.* 60% of the theoretical limit (11.7 μ_B). If antiferromagnetic interactions were dominant, the experimentally measured magnetisation would be approximately one third of the theoretical value and the $\chi_m T$ product at 1.8 K would approach one third of the value at 300 K. Hence the measured value of 7.1 μ_B indicates antiferromagnetic interactions are relatively small for this system. Part of the gradual decrease in the $\chi_m T(T)$ profile is likely to originate from the single-ion nature of the spatially separated Co^{II} centres. To evaluate the zero-field splitting (ZFS) of the Co^{II} ions, simulations were performed using MAGPACK[60,61] to better comprehend the magnetic properties of **C3**.

An approximation based on a three-fold symmetry is applied to the magnetic analysis, to avoid overparameterization. Optimization of the ZFS D value for each cobalt(II) ion with neglecting any E value gave $D/k_B = 65$ K with $g_{avg} = 2.55$. Calculated $\chi_m T(T)$ and $M(H)$ profiles reproduced the experimental results well (the solid lines superposed in Fig. 9). This D value is relatively large, but possible in comparison with the literature values.[62–65] The large D value seems to be related to the five-coordinate cobalt(II) ion (Co4, Fig. 5). On the other hand, the exchange coupling model using a spin-Hamiltonian based on an antiferromagnetic triangle, $H = -2J(S_1S_2 + S_2S_3 + S_3S_1)$, cannot reproduce the experimental M–H data (Fig. S2b, ESI†).

Conclusions

Four new non-macrocyclic heterometallic triangular $Co^{II}{}_3Ln^{III}$ clusters have been prepared by the 1 : 3:3 reaction of $Dy(NO_3)_3\cdot 6H_2O$, $Gd(NO_3)_3\cdot 6H_2O$, $La(OAc)_3\cdot 6H_2O$, or $TbCl_3\cdot 6H_2O$ with $Co(NO_3)_2\cdot 6H_2O$ and H_2**L** in methanol. Single-crystal X-ray diffraction quality crystals were obtained by the vapour diffusion of diethyl ether into concentrated methanolic solutions of **C1–C4**, allowing complete and unambiguous structural characterisation. The coordination geometry of each metal centre was examined by continuous shape measurements (CShM) using the SHAPE software package as well as OctaDist to calculate a series of octahedral distortion parameters. While **C1** was found to contain three near-perfectly octahedral Co^{II} centres, the remaining three complexes each contained one non-octahedral Co^{II} ion. This non-octahedral site was found to be strongly distorted towards trigonal prismatic in **C2**, with five coordinate centres observed for **C3**, trigonal bipyramidal, and **C4**, square pyramidal. The magnetic study of **C3** clarified a ground-state spin projection of $S_{Tot} = 3/2$ where antiferromagnetic contributions to the Co–Co interactions are weak. Throughout the literature, magnetic characterisation for the macrocyclic analogues of this type of complexes have been limited to Ni^{II}, Cu^{II}, and Zn^{II} with d^8, d^9, and d^{10} electron configurations, respectively. While the Co^{II} based systems reported here do not crystallise with the same regularity (in terms of local coordination geometries) as previously published families of macrocyclic analogues, their potentially unique magnetic properties make for an interesting avenue of research, particularly with the inclusion of high spin d^7 metal centres.

Author contributions

T. N. D., conceptualisation, investigation, data curation, formal analysis, visualisation, writing – original draft, writing – review & editing. R. T., magnetic measurements, analysis, simulation, and manuscript preparation of the magnetic data interpretation. T. I., supervision, investigation, data curation, formal analysis, writing – review & editing. P. G. P, supervision, project administration, writing – review & editing.

Conflicts of interest

There are no conflicts of interest to declare.

Acknowledgements

T. N. D. and P. G. P. would like to thank Massey University for the award of a Massey University Doctoral Scholarship for Māori to T. N. D., T. I. is grateful to the support from JSPS KAKENHI (JP20K21170 and JP17H06371).

Notes and references

1 C. O. Dietrich-Buchecker, J. P. Sauvage and J. M. Kern, *J. Am. Chem. Soc.*, 1984, **106**, 3043–3045.
2 C. Dietrich-Buchecker and J.-P. Sauvage, *Tetrahedron*, 1990, **46**, 503–512.
3 C. Dietrich-Buchecker, G. Rapenne and J.-P. Sauvage, *Coord. Chem. Rev.*, 1999, **185–186**, 167–176.
4 J. D. Crowley, S. M. Goldup, A.-L. Lee, D. A. Leigh and R. T. McBurney, *Chem. Soc. Rev.*, 2009, **38**, 1530–1541.
5 S. M. Goldup, D. A. Leigh, T. Long, P. R. McGonigal, M. D. Symes and J. Wu, *J. Am. Chem. Soc.*, 2009, **131**, 15924–15929.
6 J.-F. Ayme, J. Lux, J.-P. Sauvage and A. Sour, *Chem. –Eur. J.*, 2012, **18**, 5565–5573.
7 M. Denis and S. M. Goldup, *Nat. Rev. Chem.*, 2017, **1**, 1–17.
8 S. Yang, A. Miyachi, T. Matsuno, H. Muto, H. Sasakawa, K. Ikemoto and H. Isobe, *J. Am. Chem. Soc.*, 2021, **143**, 15017–15021.
9 N. K. Kaushik, A. Mishra, A. Ali, J. S. Adhikari, A. K. Verma and R. Gupta, *J. Biol. Inorg Chem.*, 2012, **17**, 1217–1230.
10 G.-Y. Wu, X. Shi, H. Phan, H. Qu, Y.-X. Hu, G.-Q. Yin, X.-L. Zhao, X. Li, L. Xu, Q. Yu and H.-B. Yang, *Nat. Commun.*, 2020, **11**, 3178.
11 J. Ren, X. Wei, R. Xu, Z. Chen, J. Wang, M. Wang, T. Sun, M. Wang and Y. Tang, *J. Mol. Struct.*, 2021, **1229**, 129783.
12 C.-F. Lee, D. A. Leigh, R. G. Pritchard, D. Schultz, S. J. Teat, G. A. Timco and R. E. P. Winpenny, *Nature*, 2009, **458**, 314–318.
13 X. Chen, S. Yeganeh, L. Qin, S. Li, C. Xue, A. B. Braunschweig, G. C. Schatz, M. A. Ratner and C. A. Mirkin, *Nano Lett.*, 2009, **9**, 3974–3979.
14 C. Schouwey, M. Papmeyer, R. Scopelliti and K. Severin, *Dalton Trans.*, 2015, **44**, 2252–2258.
15 H. Li, Z.-J. Yao, D. Liu and G.-X. Jin, *Coord. Chem. Rev.*, 2015, **293–294**, 139–157.
16 P. Buchwalter, J. Rosé and P. Braunstein, *Chem. Rev.*, 2015, **115**, 28–126.
17 D. Bansal, S. Pandey, G. Hundal and R. Gupta, *New J. Chem.*, 2015, **39**, 9772–9781.
18 J.-J. Du, X. Zhang, X.-P. Zhou and D. Li, *Inorg. Chem. Front.*, 2018, **5**, 2772–2776.
19 X.-R. Wu, S.-Y. Yao, L.-Q. Wei, L.-P. Li and B.-H. Ye, *Inorg. Chim. Acta*, 2018, **482**, 605–611.
20 V. Chandrasekhar, P. Bag, W. Kroener, K. Gieb and P. Müller, *Inorg. Chem.*, 2013, **52**, 13078–13086.
21 J.-L. Liu, J.-Y. Wu, Y.-C. Chen, V. Mereacre, A. K. Powell, L. Ungur, L. F. Chibotaru, X.-M. Chen and M.-L. Tong, *Angew. Chem., Int. Ed.*, 2014, **53**, 12966–12970.
22 Y. Ida, S. Ghosh, A. Ghosh, H. Nojiri and T. Ishida, *Inorg. Chem.*, 2015, **54**, 9543–9555.
23 S. Zhang, H. Li, E. Duan, Z. Han, L. Li, J. Tang, W. Shi and P. Cheng, *Inorg. Chem.*, 2016, **55**, 1202–1207.
24 L. R. Piquer and E. Carolina Sañudo, *Dalton Trans.*, 2015, **44**, 8771–8780.
25 H.-L. Wang, Z.-H. Zhu, J.-M. Peng and H.-H. Zou, *J. Clust. Sci.*, DOI: 10.1007/s10876-021-02084-7.
26 J. M. Clemente-Juan, E. Coronado and A. Gaita-Ariño, *Chem. Soc. Rev.*, 2012, **41**, 7464–7478.
27 D. Dong, *Philos. Mag.*, 2015, **95**, 2948–2954.
28 E. Macaluso, M. Rubín, D. Aguilà, A. Chiesa, L. A. Barrios, J. I. Martínez, P. J. Alonso, O. Roubeau, F. Luis, G. Aromí and S. Carretta, *Chem. Sci.*, 2020, **11**, 10337–10343.
29 S. V. Rao, J. M. Ashtree and A. Soncini, *Phys. B*, 2020, **592**, 412237.
30 D. Asthana, S. J. Lockyer, S. Nawaz, R. J. Woolfson, G. A. Timco, C. A. Muryn, I. J. Vitorica-Yrezabal, D. Collison, N. A. Burton and R. E. P. Winpenny, *Dalton Trans.*, 2021, **50**, 4390–4395.
31 S. Akine, S. Sunaga, T. Taniguchi, H. Miyazaki and T. Nabeshima, *Inorg. Chem.*, 2007, **46**, 2959–2961.
32 S. Akine, T. Taniguchi and T. Nabeshima, *Tetrahedron Lett.*, 2001, **42**, 8861–8864.
33 H. L. C. Feltham, Y. Lan, F. Kloewer, L. Ungur, L. F. Chibotaru, A. K. Powell and S. Brooker, *Chem. –Eur. J.*, 2011, **17**, 4362–4365, S4362/1-S4362/9.
34 H. L. C. Feltham, F. Kloewer, S. A. Cameron, D. S. Larsen, Y. Lan, M. Tropiano, S. Faulkner, A. K. Powell and S. Brooker, *Dalton Trans.*, 2011, **40**, 11425–11432.
35 S. Akine, S. Sunaga and T. Nabeshima, *Chem. –Eur. J.*, 2011, **17**, 6853–6861.
36 A. Yamashita, A. Watanabe, S. Akine, T. Nabeshima, M. Nakano, T. Yamamura and T. Kajiwara, *Angew. Chem.*, 2011, **50**, 4016–4019, S4016/1-S4016/5.
37 H. Nagae, R. Aoki, S. Akutagawa, J. Kleemann, R. Tagawa, T. Schindler, G. Choi, T. P. Spaniol, H. Tsurugi, J. Okuda and K. Mashima, *Angew. Chem., Int. Ed.*, 2018, **57**, 2492–2496.
38 M. Yamamura, M. Sasaki, M. Kyotani, H. Orita and T. Nabeshima, *Chem. –Eur. J.*, 2010, **16**, 10638–10643.
39 M. Yamamura, M. Iida, K. Kanazawa, M. Sasaki and T. Nabeshima, *Bull. Chem. Soc. Jpn.*, 2014, **87**, 334–340.
40 W. A. Rabanal-León, J. A. Murillo-López and R. Arratia-Pérez, *Phys. Chem. Chem. Phys.*, 2016, **18**, 33218–33225.
41 H. L. C. Feltham, R. Clerac, A. K. Powell and S. Brooker, *Inorg. Chem.*, 2011, **50**, 4232–4234.
42 H. L. C. Feltham, R. Clerac, L. Ungur, V. Vieru, L. F. Chibotaru, A. K. Powell and S. Brooker, *Inorg. Chem.*, 2012, **51**, 10603–10612.
43 H. L. C. Feltham, R. Clerac, L. Ungur, L. F. Chibotaru, A. K. Powell and S. Brooker, *Inorg. Chem.*, 2013, **52**, 3236–3240.
44 S. Dhers, H. L. C. Feltham, R. Clerac and S. Brooker, *Inorg. Chem.*, 2013, **52**, 13685–13691.
45 S. Dhers, H. L. C. Feltham, M. Rouzieres, R. Clerac and S. Brooker, *Dalton Trans.*, 2016, **45**, 18089–18093.

46 S. Dhers, H. L. C. Feltham, M. Rouzieres, R. Clerac and S. Brooker, *Inorg. Chem.*, 2019, **58**, 5543–5554.
47 H. L. C. Feltham, S. Dhers, M. Rouzieres, R. Clerac, A. K. Powell and S. Brooker, *Inorg. Chem. Front.*, 2015, **2**, 982–990.
48 H. Asaba, T. Iwasaki, M. Hatazawa, J. Deng, H. Nagae, K. Mashima and K. Nozaki, *Inorg. Chem.*, 2020, **59**, 7928–7933.
49 T. N. Dais, R. Takano, T. Ishida and P. G. Plieger, *Dalton Trans.*, 2022, **51**, 1446–1453.
50 A. J. Gallant, J. H. Chong and M. J. MacLachlan, *Inorg. Chem.*, 2006, **45**, 5248–5250.
51 T. Nabeshima, H. Miyazaki, A. Iwasaki, S. Akine, T. Saiki, C. Ikeda and S. Sato, *Chem. Lett.*, 2006, **35**, 1070–1071.
52 D. Casanova, J. Cirera, M. Llunell, P. Alemany, D. Avnir and S. Alvarez, *J. Am. Chem. Soc.*, 2004, **126**, 1755–1763.
53 M. Pinsky and D. Avnir, *Inorg. Chem.*, 1998, **37**, 5575–5582.
54 R. Ketkaew, Y. Tantirungrotechai, P. Harding, G. Chastanet, P. Guionneau, M. Marchivie and D. J. Harding, *Dalton Trans.*, 2021, **50**, 1086–1096.
55 N. E. Brese and M. O'Keeffe, *Acta Crystallogr. B*, 1991, **47**, 192–197.
56 I. D. Brown, *Chem. Rev.*, 2009, **109**, 6858–6919.
57 A. L. Spek, *J. Appl. Crystallogr.*, 2003, **36**, 7–13.
58 A. L. Spek, *Acta Crystallogr., Sect. D: Biol. Crystallogr.*, 2009, **65**, 148–155.
59 O. V. Dolomanov, L. J. Bourhis, R. J. Gildea, J. A. Howard and H. Puschmann, *J. Appl. Crystallogr.*, 2009, **42**, 339–341.
60 J. Borrás-Almenar, J. Clemente-Juan, E. Coronado and B. Tsukerblat, *Inorg. Chem.*, 1999, **38**, 6081–6088.
61 J. Borrás-Almenar, J. M. Clemente-Juan, E. Coronado and B. S. Tsukerblat, *J. Comput. Chem.*, 2001, **22**, 985–991.
62 T. Yamane, K. Sugisaki, H. Matsuoka, K. Sato, K. Toyota, D. Shiomi and T. Takui, *Dalton Trans.*, 2018, **47**, 16429–16444.
63 G. Novitchi, S. Jiang, S. Shova, F. Rida, I. Hlavička, M. Orlita, W. Wernsdorfer, R. Hamze, C. Martins, N. Suaud, N. Guihéry, A.-L. Barra and C. Train, *Inorg. Chem.*, 2017, **56**, 14809–14822.
64 B. Papánková, R. Boča, Ľ. Dlháň, I. Nemec, J. Titiš, I. Svoboda and H. Fuess, *Inorg. Chim. Acta*, 2010, **363**, 147–156.
65 J. Zhou, J. Song, A. Yuan, Z. Wang, L. Chen and Z.-W. Ouyang, *Inorg. Chim. Acta*, 2018, **479**, 113–119.